

Supporting Information

Immobilization of europium and terbium ions with tunable ratios on a dispersible two-dimensional metal–organic framework for ratiometric photoluminescent detection of D₂O

Tzu-Chi Lin,^a Kuan-Chu Wu,^a Jhe-Wei Chang,^a You-Liang Chen,^a Meng-Dian Tsai^a and Chung-Wei Kung^{*a}

^a Department of Chemical Engineering, National Cheng Kung University, Tainan City, Taiwan, 70101.

*Email: cwkung@mail.ncku.edu.tw

Table S1. Amounts of precursors dissolved in 12 mL of DMF used for the installation of lanthanide ions in 30 mg of ZrBTB.

Obtained material	Eu(OAc) ₃ (mg)	Tb(OAc) ₃ (mg)
Eu-ZrBTB	96.5	0
Eu-Tb-ZrBTB(1:1)	48.2	49.3
Eu-Tb-ZrBTB(1:5)	16.1	82.1
Eu-Tb-ZrBTB(1:10)	8.8	89.6
Eu-Tb-ZrBTB(1:20)	4.6	93.8
Eu-Tb-ZrBTB(1:30)	3.1	95.3
Tb-ZrBTB	0	98.5

Table S2. ICP-OES results.

Material	Eu atom per hexa-zirconium node	Tb atom per hexa-zirconium node
Eu-ZrBTB	4.2	-
Eu-Tb-ZrBTB(1:1)	2.4	2.6
Eu-Tb-ZrBTB(1:5)	0.8	4.0
Eu-Tb-ZrBTB(1:10)	0.4	4.4
Eu-Tb-ZrBTB(1:20)	0.2	4.5
Eu-Tb-ZrBTB(1:30)	0.1	4.2
Tb-ZrBTB	-	4.5

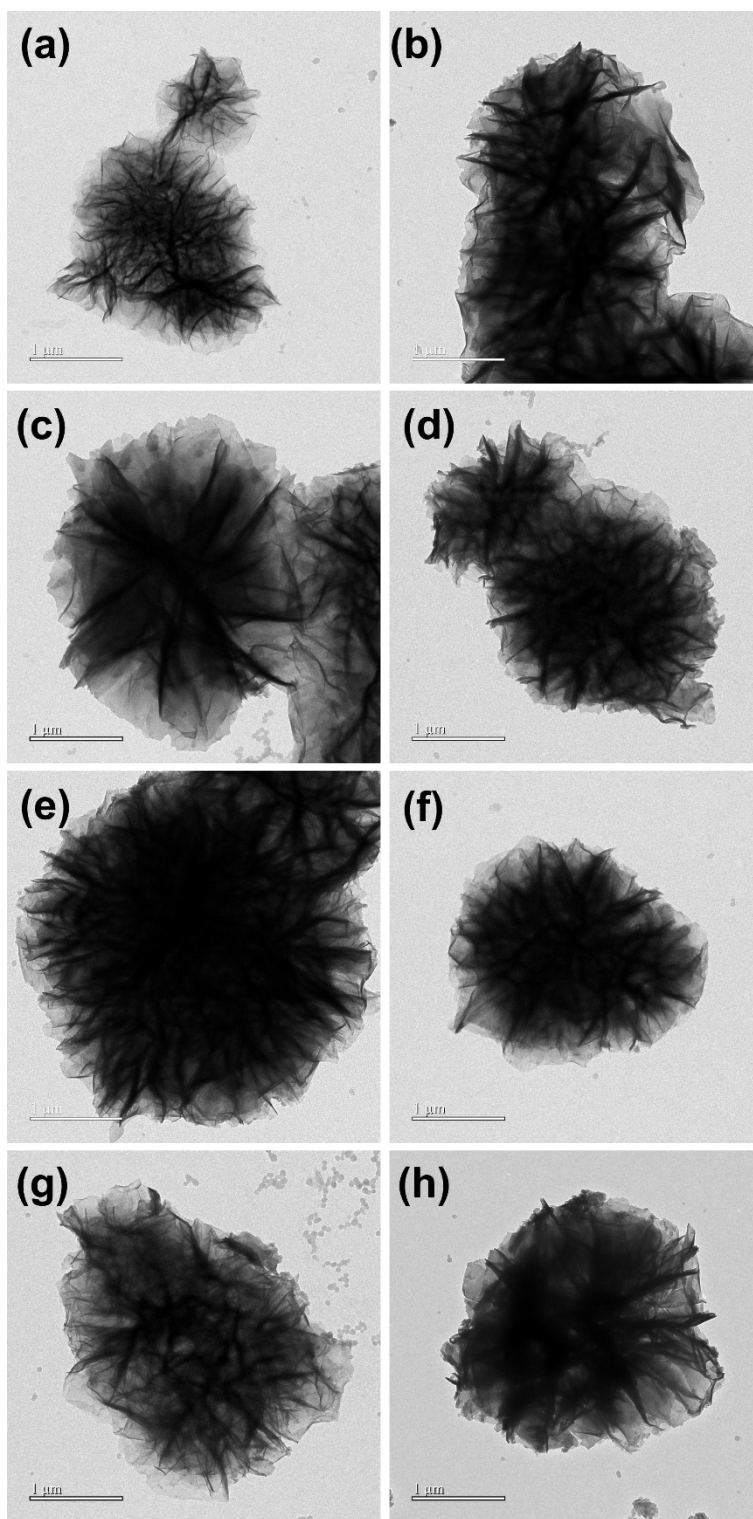


Figure S1. TEM images of (a) ZrBTB, (b) Tb-ZrBTB, (c) Eu-Tb-ZrBTB(1:30), (d) Eu-Tb-ZrBTB(1:20), (e) Eu-Tb-ZrBTB(1:10), (f) Eu-Tb-ZrBTB(1:5), (g) Eu-Tb-ZrBTB(1:1) and (h) Eu-ZrBTB, collected at a low magnification (scale bar = 1 μm).

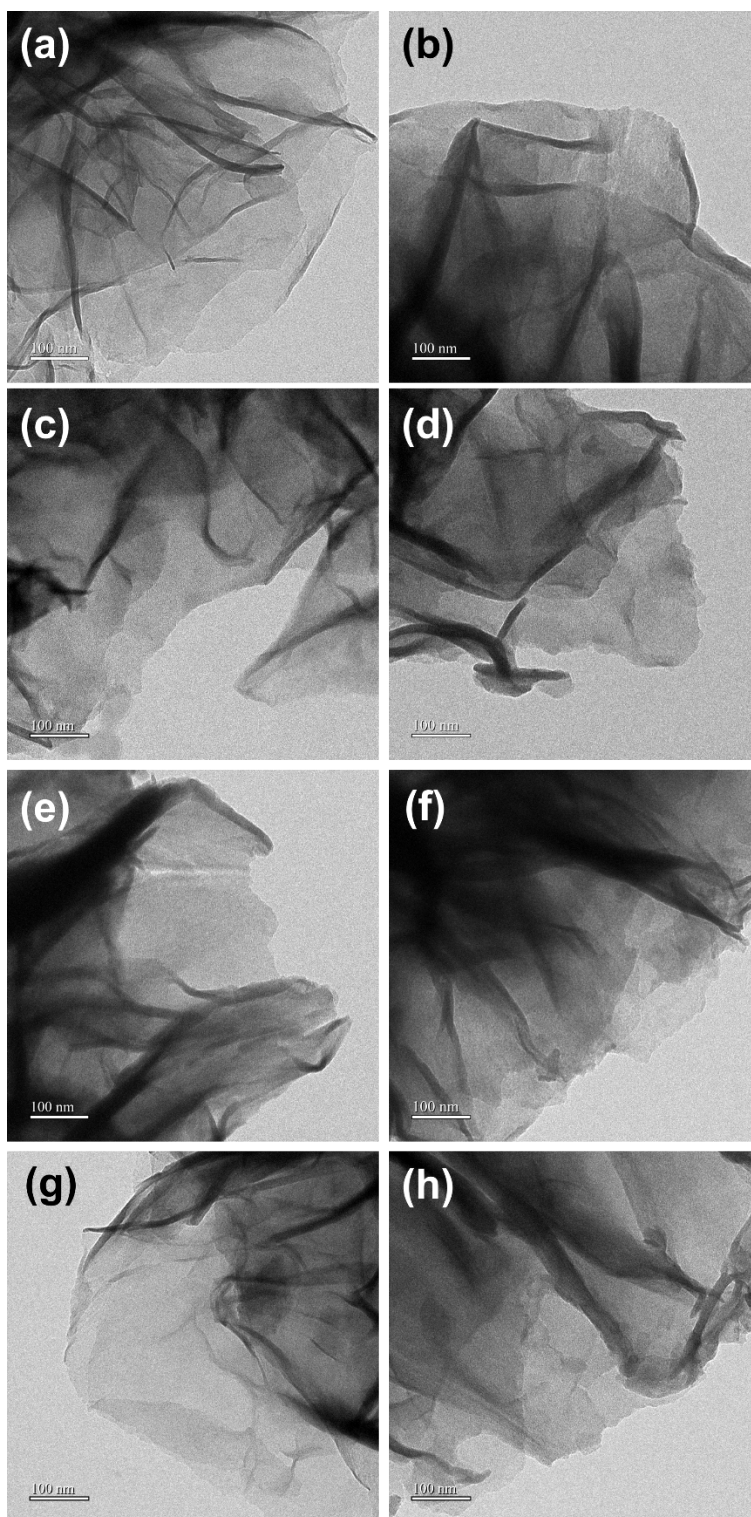


Figure S2. TEM images of (a) ZrBTB, (b) Tb-ZrBTB, (c) Eu-Tb-ZrBTB(1:30), (d) Eu-Tb-ZrBTB(1:20), (e) Eu-Tb-ZrBTB(1:10), (f) Eu-Tb-ZrBTB(1:5), (g) Eu-Tb-ZrBTB(1:1) and (h) Eu-ZrBTB, collected at a high magnification (scale bar = 100 nm).

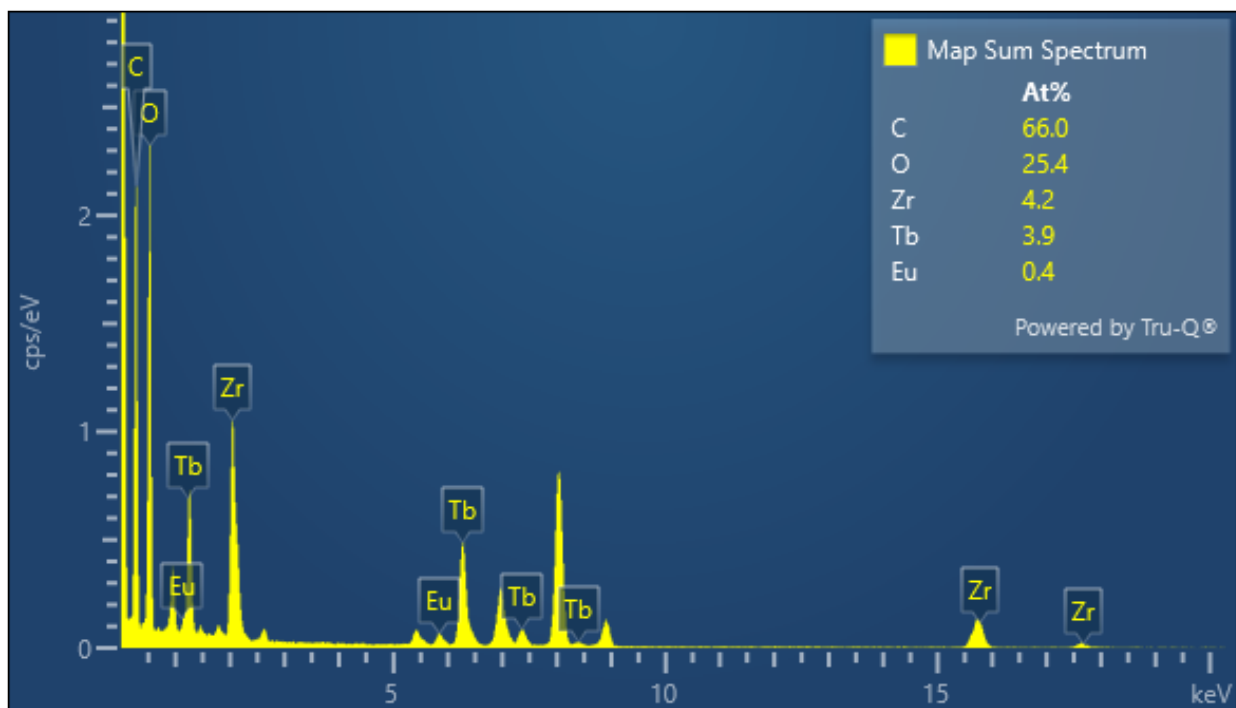


Figure S3. Representative EDS spectrum of Eu-Tb-ZrBTB(1:10).

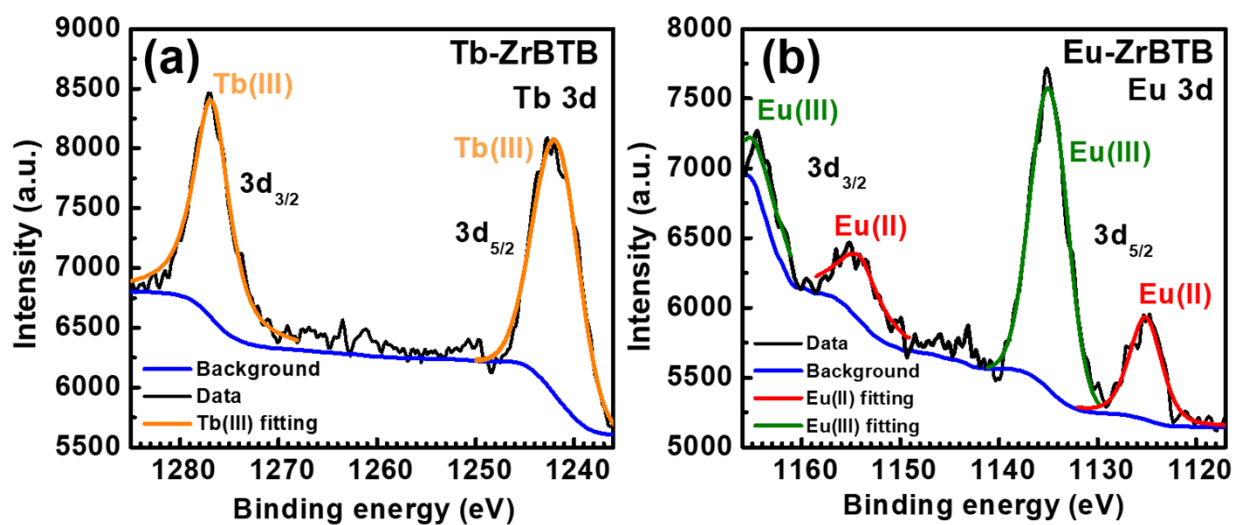


Figure S4. High-resolution XPS spectra of (a) Tb-ZrBTB in the region of Tb 3d and (b) Eu-ZrBTB in the region of Eu 3d.

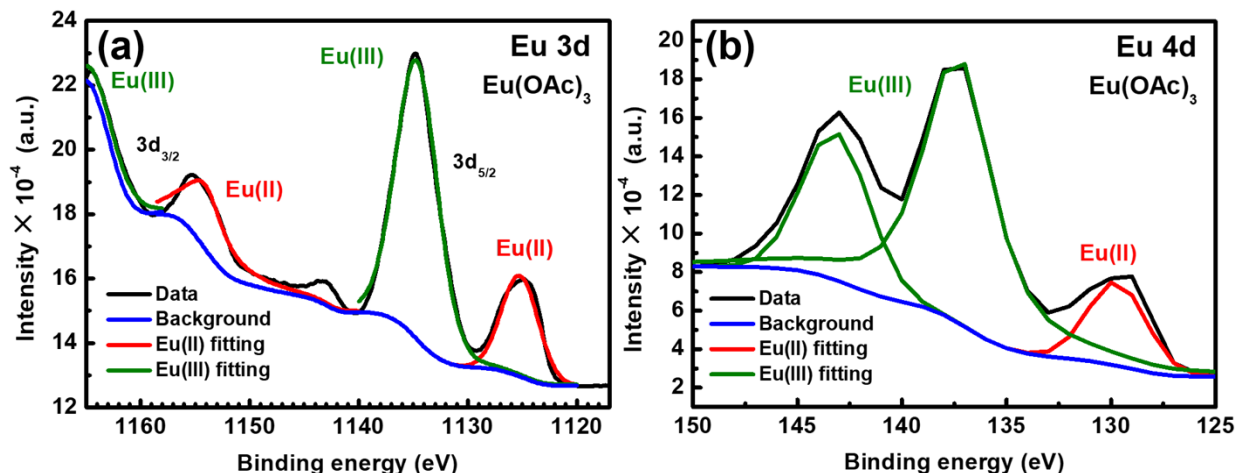


Figure S5. High-resolution XPS spectra of $\text{Eu}(\text{OAc})_3$ collected in the regions of (a) Eu 3d and (b) Eu 4d.

It has been reported that under the excitation of the BTB linker, energy transfer can occur from the BTB linker to the installed terbium ion in Tb-ZrBTB to amplify the PL emission of terbium, with the maximum emission peak located at around 543 nm.¹ In addition, as shown in Figure 5(a) in the main text, significant PL emission of installed europium ions with the maximum emission peak located at around 613 nm can also be observed for Eu-ZrBTB under the excitation of the BTB linker, suggesting the energy transfer from the BTB linker to the installed europium ion as well. Thus, to find the optimal wavelength for the excitation of the BTB linker, excitation spectra of the suspensions of Tb-ZrBTB and Eu-ZrBTB were first collected by examining the PL emissions of terbium and europium at 543 nm and 613 nm, respectively. As shown in Figure S6, both the maximum emission of terbium for Tb-ZrBTB and that of europium for Eu-ZrBTB can be achieved under the excitation of the BTB linker at around 320 nm. Thus, 320 nm was selected as the excitation wavelength for all PL measurements in this study.

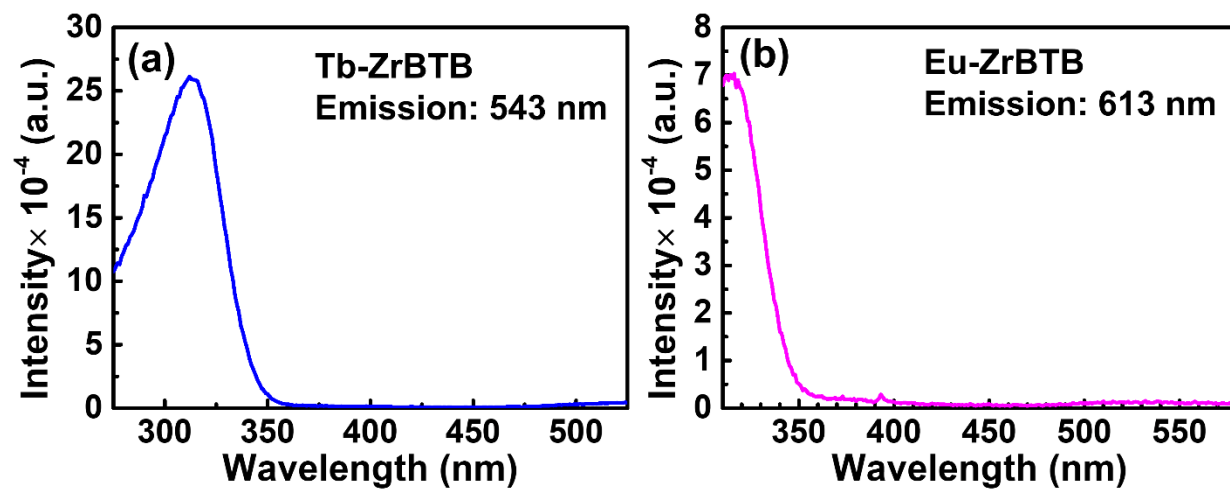


Figure S6. Excitation spectra of the suspensions of (a) Tb-ZrBTB and (b) Eu-ZrBTB, with a concentration of 0.2 mg/mL. Emission was collected at 543 nm and 613 nm for Tb-ZrBTB and Eu-ZrBTB, respectively.

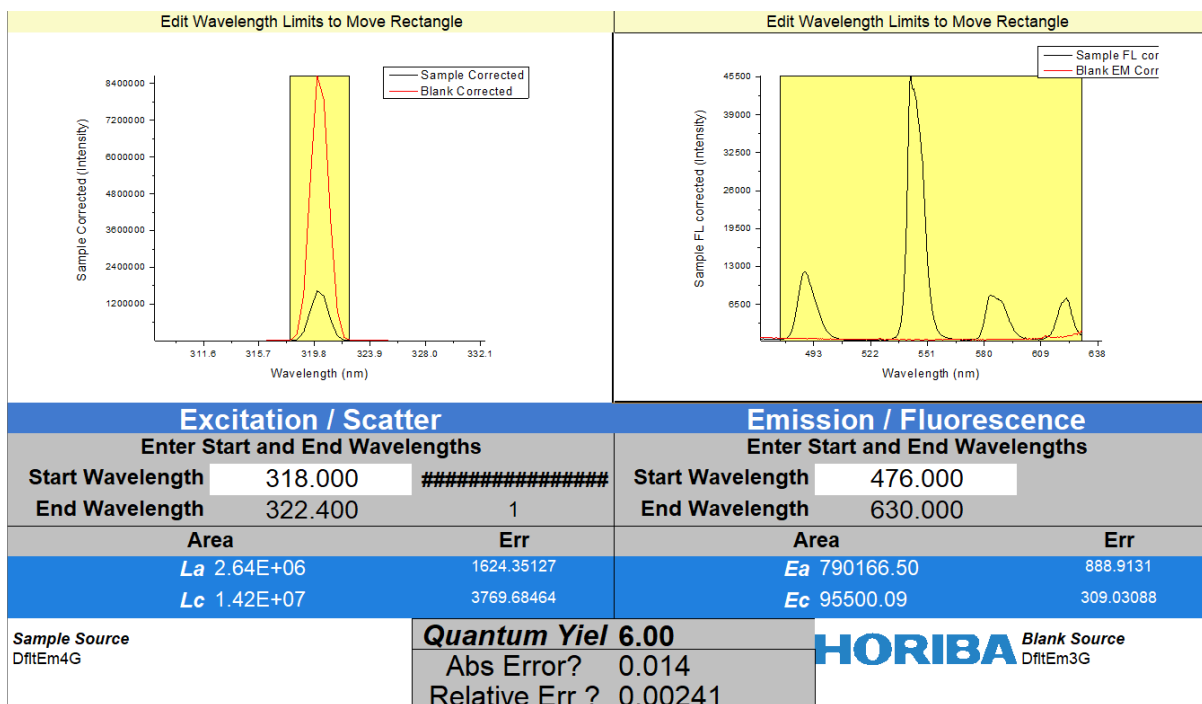


Figure S7. Data of the PLQY measurement for the Tb-ZrBTB solid powder, under the excitation at 320 nm. Emissions of lanthanide ions between 476 nm and 630 nm were all considered.

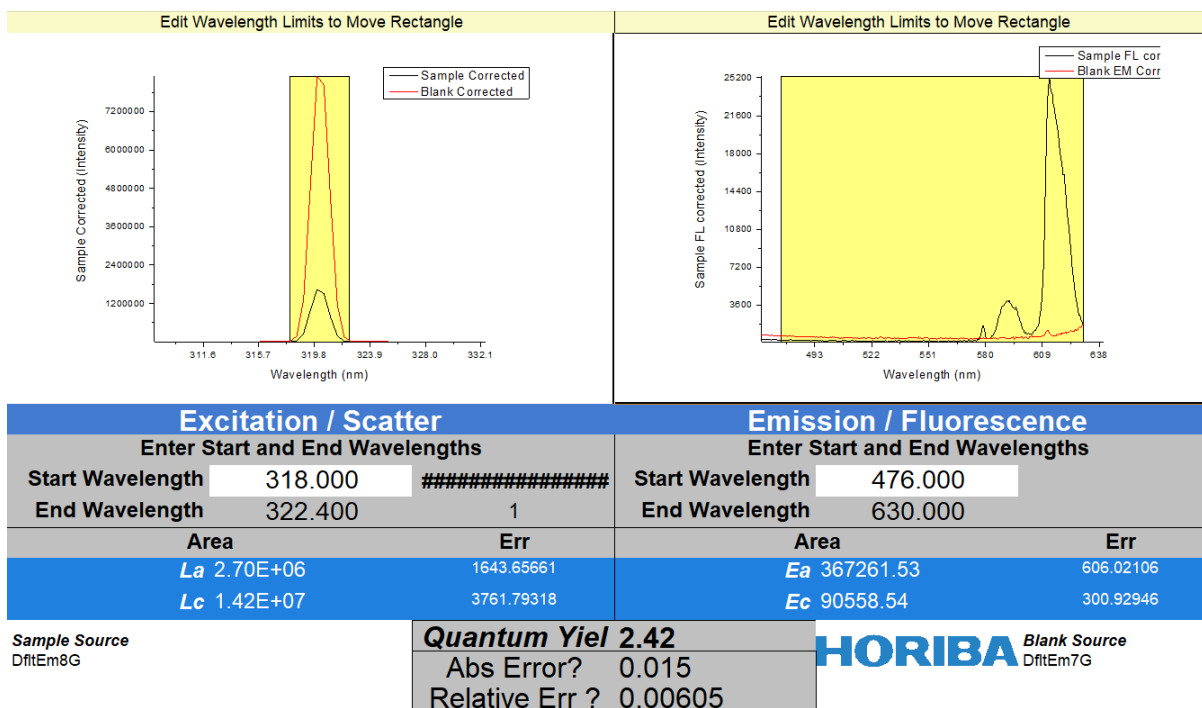


Figure S8. Data of the PLQY measurement for the Eu-ZrBTB solid powder, under the excitation at 320 nm. Emissions of lanthanide ions between 476 nm and 630 nm were all considered.

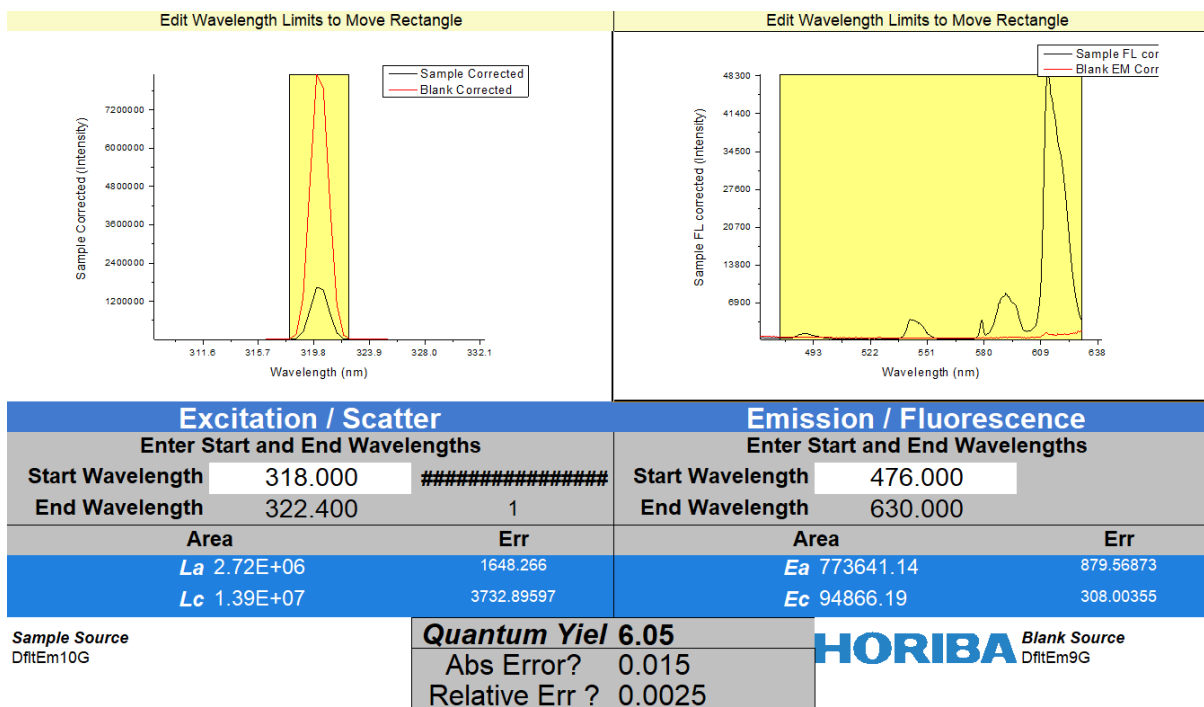


Figure S9. Data of the PLQY measurement for the Eu-Tb-ZrBTB(1:10) solid powder, under the excitation at 320 nm. Emissions of lanthanide ions between 476 nm and 630 nm were considered.

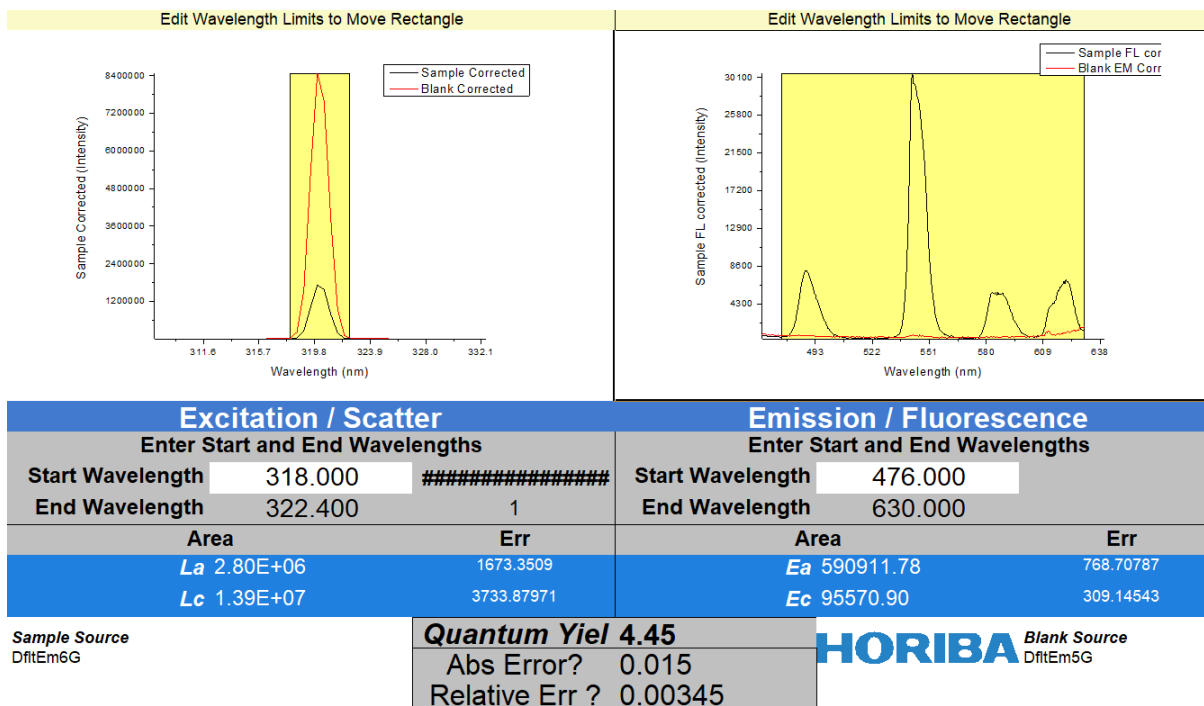


Figure S10. Data of PLQY measurement for Eu-ZrBTB/Tb-ZrBTB(1:10) solid powder, under the excitation at 320 nm. Emissions of lanthanide ions between 476 nm and 630 nm were considered.

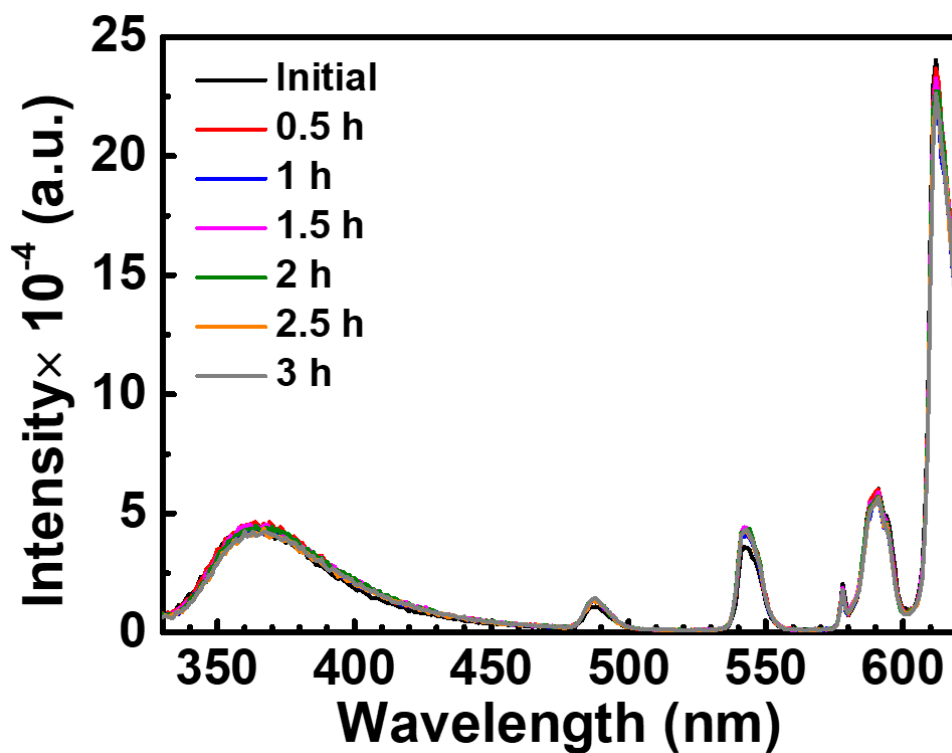


Figure S11. Emission spectra of the suspension of Eu-Tb-ZrBTB(1:10) with a concentration of 0.2 mg/mL in the ethanol/water (1:1) mixture, collected during three hours of the long-term stability test. Excitation wavelength: 320 nm.

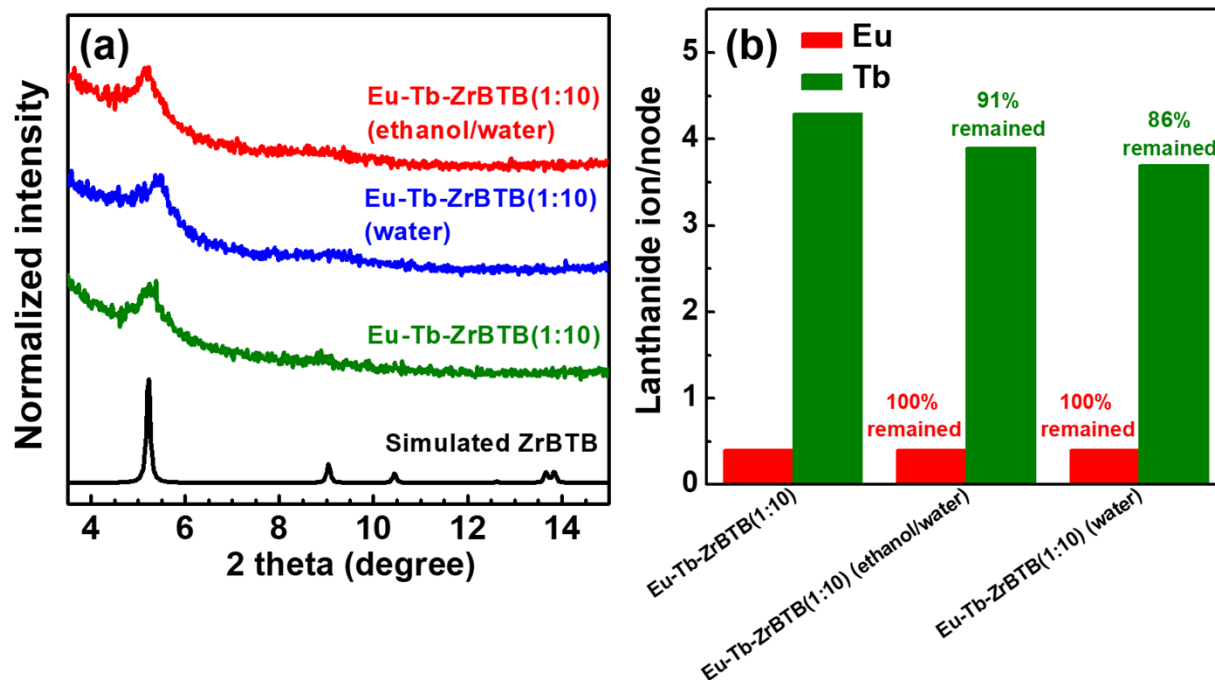


Figure S12. Testing results for the chemical stability of Eu-Tb-ZrBTB(1:10). Eu-Tb-ZrBTB(1:10) was dispersed in the ethanol/water (1:1) mixture and pure water with a concentration of 0.2 mg/mL, respectively. After 1 h of exposure, the MOF solid was collected by centrifugation, washed with the solvent used for preparing the corresponding suspension, and subjected to the solvent exchange with acetone for three times over the course of overnight. The thermally activated samples were named as Eu-Tb-ZrBTB(1:10) (ethanol/water) and Eu-Tb-ZrBTB(1:10) (water), respectively. (a) XRD patterns and (b) ICP-OES results of the fresh Eu-Tb-ZrBTB(1:10), Eu-Tb-ZrBTB(1:10) (ethanol/water) and Eu-Tb-ZrBTB(1:10) (water).

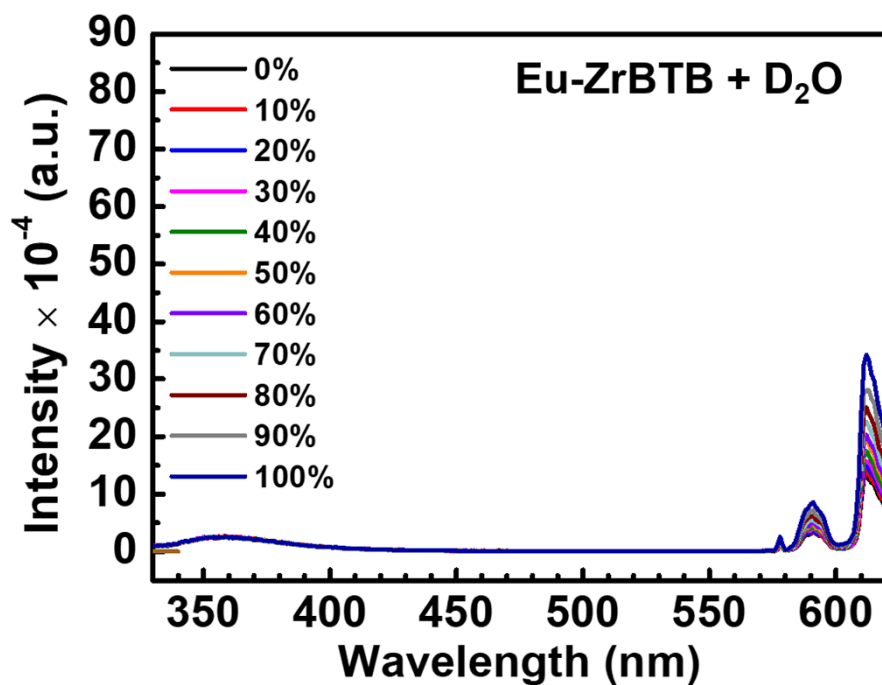


Figure S13. Emission spectra of the suspensions of Eu-ZrBTB collected during the sensing experiments. Excitation wavelength: 320 nm.

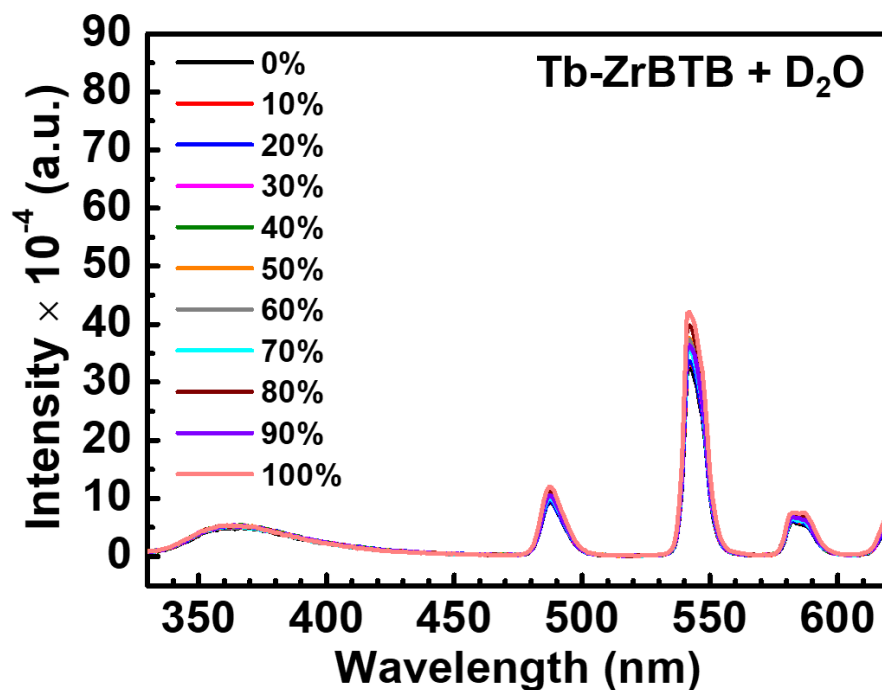


Figure S14. Emission spectra of the suspensions of Tb-ZrBTB collected during the sensing experiments. Excitation wavelength: 320 nm.

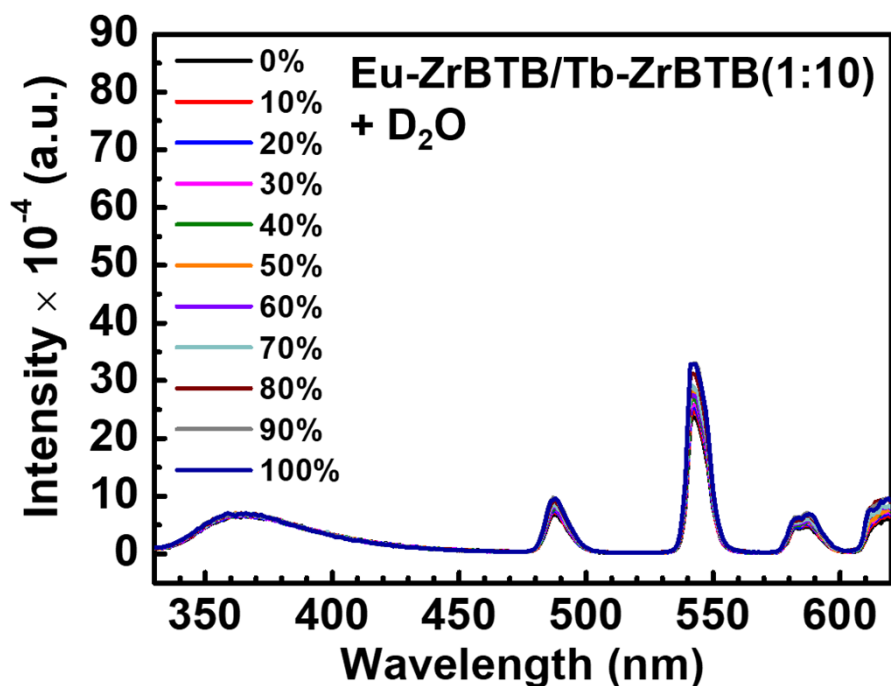


Figure S15. Emission spectra of the suspensions of Eu-ZrBTB/Tb-ZrBTB(1:10) collected during the sensing experiments. Excitation wavelength: 320 nm.

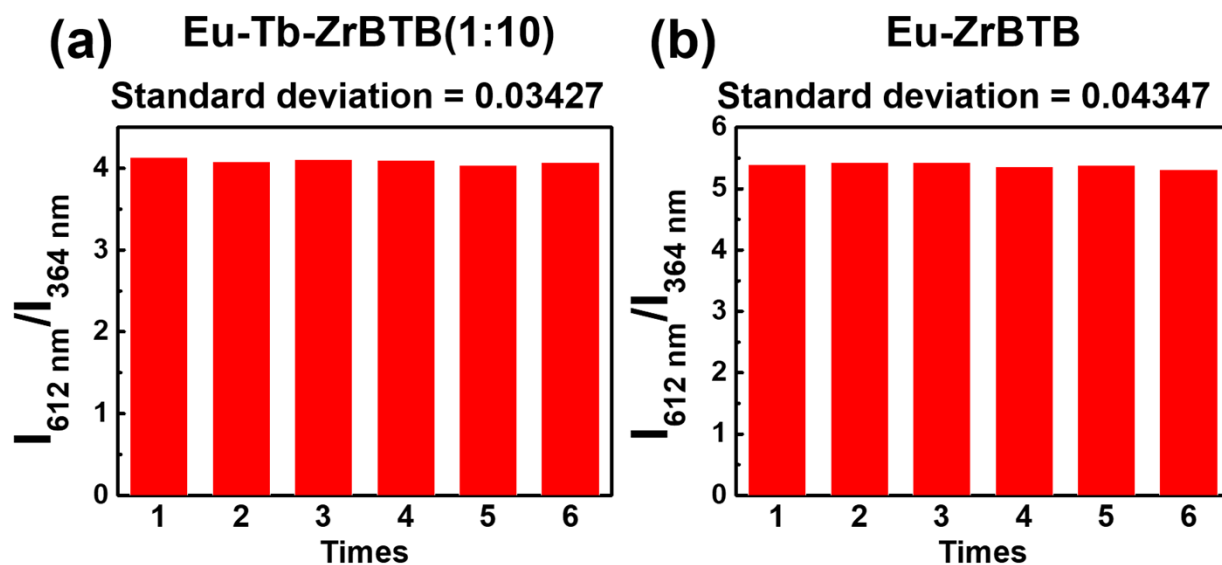


Figure S16. $I_{612 \text{ nm}}/I_{364 \text{ nm}}$ collected under the excitation at 320 nm from six parallel experiments with suspensions of (a) Eu-Tb-ZrBTB(1:10) and (b) Eu-ZrBTB without adding D_2O .

Table S3. Comparison between LOD values of lanthanide-based materials reported for D₂O detection.

Material	LOD (wt%)	Reference
Uranyl–europium framework (SCU-UEu-1)	<1%	[2]
Ln(III) -based MOF (Eu _{0.5} Tb _{0.5} -TZB-MOF)	0.111%	[3]
Ln-MOF(Ce/Eu@Gd-MOF)	0.001%	[4]
Eu-Tb-ZrBTB(1:10)	1.13%	This work
Eu-ZrBTB	1.78%	

Reference:

1. Y.-L. Chen, C.-H. Shen, C.-W. Huang and C.-W. Kung, *Mol. Syst. Des. Eng.*, 2023, **8**, 330-340.
2. Y. Zhang, L. Chen, Z. Liu, W. Liu, M. Yuan, J. Shu, N. Wang, L. He, J. Zhang, J. Xie, X. Chen and J. Diwu, *ACS Appl. Mater. Interfaces*, 2020, **12**, 16648-16654.
3. J. Xiong, Y. Chen, S. Li, X. Tan, L. Wang, J. Chen, Q. Luo, Q. Gao, X. Tong and F. Luo, *Inorg. Chem.*, 2024, **63**, 4269-4278.
4. X. Fan, Z. Guo, X. Wen, W. Liu, B. Guan, F. Yin, X. Hong, T. Tan, K. Wang and J. Wang, *J. Mater. Chem. C*, 2024, **12**, 868-873.